

Layer-by-layer assembly of polymers and anisotropic nanomaterials using spray-based approach

Souvik De^{1,2,a)}, Anish Patel², Jodie L. Lutkenhaus^{2,3}

Received: 20 October 2019; accepted: 5 February 2020

Traditional dip-assisted layer-by-layer (LbL) assembly produces robust and conformal coatings, but it is time-consuming. Alternatively, spray-assisted layer-by-layer (SA-LbL) assembly has gained interest due to rapid processing resulting from the short adsorption time. However, it is challenging to assemble anisotropic nanomaterials using this spray-based approach. This is because the standard approach for fabricating "all-polyelectrolyte" LbL films does not necessarily give rise to satisfactory film growth when one of the adsorbing components is anisotropic. Here, polymers are combined with a model anisotropic nanomaterial via SA-LbL assembly. Specifically, graphene oxide (GO) is investigated, and the effect of anchor layer, colloidal stability, charge distribution along the carbon framework, and concentration of polymer on the growth and the film quality is examined to gain insight into how to achieve pinhole-free, smooth polymer/GO SA-LbL coatings. This approach might be applicable to other anisotropic nanomaterials such as clays or 2D nanomaterials for future development of uniform coatings by spraying.

Introduction

After popularization by Decher et al., layer-by-layer (LbL) assembly has been regarded as one of the most promising nanofabrication techniques to produce conformal coatings from various combinations of materials on a wide range of substrates [1, 2, 3]. LbL assembly is based on the alternating adsorption of oppositely charged species onto a substrate through electrostatic interactions; other interactions such as hydrogen bonding, hydrophobic, host-guest, covalent, and stereochemical interactions are well documented [4]. Taking advantage of the environmentally friendly nature of the waterbased processing approach and the precise control over film morphology, a broad range of materials including polyelectrolytes [1], nanoparticles [5, 6, 7, 8], zeolites [9, 10], metal organic frameworks (MOF) [11], metal oxides [12, 13], and DNA [14] have been successfully assembled into LbL films onto substrates ranging from silicon to glass, plastic, and even textiles [11, 15].

The traditional and most robust LbL assembly approach is based on immersion of the substrate or dipping. In the case of

dip-assisted LbL assembly, the substrate is alternately dipped for minutes into the solutions/dispersions of complementary species. Between the deposition steps, the sample is rinsed to remove the loosely bound species from the substrate. Traditionally, dip-assisted LbL was performed by alternate dipping of the substrate for 15-20 min in the solution of complementary species [16, 17, 18, 19]. Therefore, the robustness of dipassisted LbL assembly arises from the long adsorption time, which makes the process amenable to fabricating a broad combination of materials into thin films with rates of high success. Recently, several successful dip-assisted LbL films have been fabricated with various combinations of materials with relatively shorter dipping time [20, 21, 22, 23, 24]. However, the long adsorption step results in longer processing times, which are not always desirable for real-world implementation.

Journal of Materials Research 📗 Volume 35 📄 Issue 9 🖿 May 14, 2020 📄 www.mrs.org/jmi

In this context, spray-assisted LbL (SA-LbL) assembly [19, 25], owing to fast processing (\sim 40× faster than dip-assisted LbL assembly), has emerged as an alternative. The rapid processing of SA-LbL assembly arises from the smaller diffusion

© Materials Research Society 2020 cambridge.org/JMR

¹Department of Applied Chemistry, Jabalpur Engineering College, Jabalpur, Madhya Pradesh 482011, India

²Artie McFerrin Department of Chemical Engineering, Texas A&M University, College Station, Texas 77843, USA

³Department of Materials Science & Engineering, Texas A&M University, College Station, Texas 77843, USA

^{a)}Address all correspondence to this author. e-mail: souvikiitm@gmail.com



length of the adsorbing species in the sprayed liquid droplet and wetted layer, requiring a shorter contact time. SA-LbL assembly has proven to be a robust technique to fabricate "allpolyelectrolyte" LbL films (polyelectrolyte multilayers). This is because the multiple charge sites along the polyelectrolyte chains and strong interpenetration between the deposited layers give rise to a large number of electrostatic interactions between the oppositely charged polyelectrolytes [Fig. 1(a)]. However, nano-objects such as nanoparticles, nanoplatelets, and nanorods often suffer from poor layer interpenetration due to their rigid nanostructures [Fig. 1(b)]. Consequently, successful LbL assembly of rigid nano-objects in a conformal manner requires longer exposure times or other additional fabrication steps such as drying. Additionally, owing to the short contact time and the tendency for aggregation of nano-objects, several intrinsic and extrinsic parameters become even more critical in controlling thickness, roughness, and morphology of the resulting film. Due to these challenges, their success is system-specific and no universal set of guidelines still exist for SA-LbL assembly with nano-objects [4]. Consequently, there are only a limited number of reports on SA-LbL assembly of nanomaterials [26, 27, 28, 29, 30, 31, 32, 33, 34, 35, 36, 37].

In this contribution, we systematically investigate how different intrinsic parameters affect the SA-LbL deposition process and the morphology of the resulting film when one of the adsorbing species is graphene oxide (GO). GO acts as precursor material for reduced GO, which is useful for application in electrodes for energy storage [5, 30, 38], gas barrier coatings [39, 40], anticorrosion coatings [41], smart conductive coatings [42], and sensors [43, 44]. GO has been recently assembled by SA-LbL with polyelectrolytes [45, 46, 47]. Despite these reports, a universal protocol for SA-LbL of GO with polyelectrolytes is still lacking. We start with applying the SA-LbL assembly protocol often used for polyelectrolyte multilayers and then systematically screen through parameters such as colloidal stability of the GO dispersion, charge distribution across the carbon framework, whether the presence of anchor layers facilitates the deposition process, and polymer concentration. We also show that replacing the spray rinsing step with blow-drying in between the exposure steps gives rise to uniform growth behavior. Finally, the knowledge gained from this investigation was used to develop a robust SA-LbL assembly protocol that leads to pinhole free smooth GO/ polymer coatings with uniform growth profile. With this approach, it becomes possible to fabricate high-quality GObased LbL coatings using a spray-based approach.

Result and discussion

Downloaded from https://www.cambridge.org/core. Texas A&M University Evans Libraries, on 17 Jul 2020 at 01:59:58, subject to the Cambridge Core terms of use, available at https://www.cambridge.org/core/terms. https://doi.org/10.1557/jmr.2020.44

LbL assembly of nanomaterials requires a stable dispersion and nanomaterials that carry charge or other secondary interactions

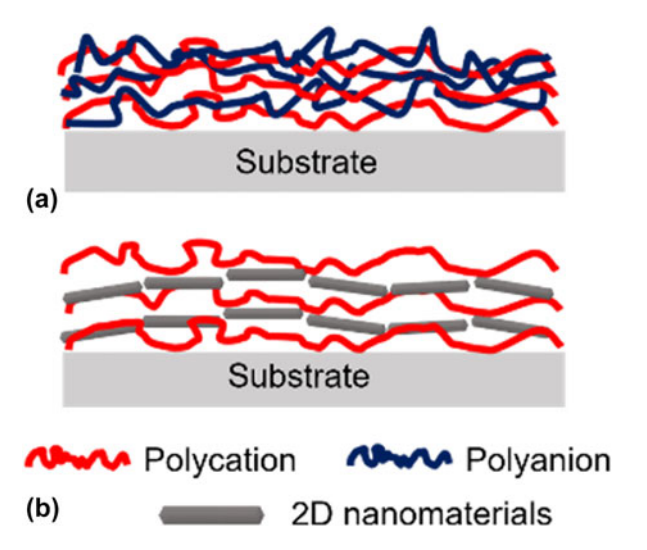


Figure 1: Schematic representation of LbL assembled coatings composed of (a) oppositely charged polyelectrolytes showing layer interpenetration and (b) polyelectrolytes and anisotropic nanomaterials showing lack of layer interpenetration.

for assembling with a complementary species [here, polydiallyldimethylammonium chloride (PDAC)]. PDAC was selected as the polyelectrolyte because it has been extensively investigated as a positively charged polyelectrolyte for dip-assisted and SA-LbL assembly [25, 48, 49, 50, 51, 52]. Both GO and edge-oxidized GO (GO_{Edge}) aqueous dispersions were prepared by first ultrasonicating, followed by bath sonication prior to use. The zeta potential of GO and GO_{Edge} at pH 3.5 was found to be -41.7 mV and -44 mV, respectively. The zeta potential values of GO_{Edge} and GO are comparable to that of poly(styrene sulfonate) (PSS), which has a zeta potential of -45 mV. Several studies demonstrated SA-LbL assembly of (PSS/PDAC) multilayer films [25, 50, 51]. Therefore, we postulated that both GO_{Edge} and GO would be suitable for SA-LbL assembly with PDAC.

When creating "all-polyelectrolyte" multilayers using SA-LbL assembly, that is, with polycations and polyanions, a common approach is to spray polyelectrolytes for 10-20 s with spray rinsing for 10-20 s in between the spray deposition steps. The process is then repeated until the desired number of layer pairs are deposited [Fig. 2(a)]. Starting with this approach, we performed SA-LbL assembly by spraying complementary species GO_{Edge} (0.5 mg/mL) and PDAC (1.0 mg/mL) for 10 s spraying and 10 s rinsing at a pressure 30 psi. The reason for choosing this pressure is that it is sufficient to produce a wetted film on the substrate [29]. However, even after 60 cycles of deposition of (PDAC/GO_{Edge}) using the aforementioned protocol, we observed a film thickness of only 5 nm, indicating no growth. Even a higher spraying time of 30 s and a rest time for 30 s between spraying and rinsing did not lead to any LbL deposition. This clearly indicates that while



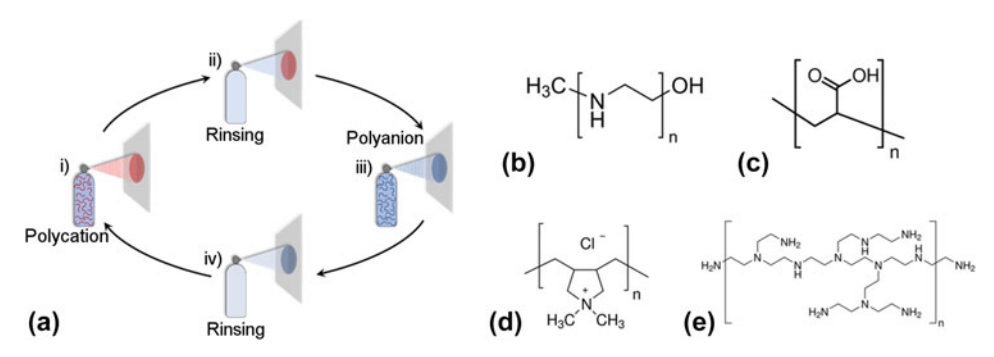


Figure 2: (a) Schematic representation of spray assisted LbL assembly for polyelectrolyte multilayers: (i) spraying of polycation on a negatively charged substrate, (ii) spray rinsing to remove excess and loosely bound polycation, (iii) spraying of polyanion, and (iv) spray rinsing to remove excess and loosely bound polyanion. The whole process constitutes a single cycle and produces a layer pair. The cycle is repeated for deposition of desired numbers of layer pair. Structure of (b) L-PEI, (c) PAA, (d) PDAC, and (e) B-PEI.

a dipping protocol for "all polyelectrolyte" works for LbL assembly of nanomaterials, the SA-LbL protocol for "all polyelectrolyte" does not necessarily give rise to satisfactory or any growth for LbL film containing nanomaterials such as GO.

A common approach for LbL assembly is to use an anchor layer or adhesion promoting layer that not only helps layer growth but also improves the adhesion of the film to the substrate. Hence, we deposited 4-layer pairs of adhesionpromoting layers of linear polyethylenimine/polyacrylic acid (L-PEI/PAA) on silicon using SA-LbL assembly (10 s spraying and 10 s rinsing) prior to LbL deposition PDAC and GO_{Edge}. The introduction of the adhesion-promoting layers led to visible deposition on the silicon substrate. However, unlike typical LbL films, the (PDAC/GO_{Edge}) SA-LbL coatings were matte in appearance, indicating inhomogeneous deposition. For instance, after 40 cycles of deposition of (PDAC/GO_{Edge})₄₀, the measured thickness and roughness of the resulting film were found to be 224 nm and 148 nm, respectively [Figs. 3(a) and 3(b)]. For comparison, we also performed dip-LbL on a silicon substrate to produce a (PDAC/GO_{Edge})₁₅ LbL film using a typical "all-polyelectrolyte" dip-assisted LbL assembly protocol. The (PDAC/GO_{Edge})₁₅ dip-LbL film showed a roughness of about 20% of the overall thickness results [Fig. 3(c)]. In contrast, for (PDAC/GO_{Edge})₂₀ SA-LBL film, the roughness increases to 60% of the overall thickness [Fig. 3(d)]. We also used a longer spraying time of 30 s with or without a rest time of 30 s between spraying and rinsing. However, both the conditions did not lead to any deposition beyond the (L-PEI/ PAA)₄ anchor layers. This indicates that longer spraying times have an adverse effect on the growth of SA-LbL films when one of the adsorbing species is an anisotropic nanomaterial. This further highlights the challenges associated with the fabrication of smooth and uniform LbL coatings containing nano-objects using a spray-based approach.

We hypothesized that the inhomogeneous deposition in the case of SA-LbL assembly with 10 s spray and 10 s rinsing might

result from the spray-rinsing occurring after spray deposition steps. Rigid anisotropic nanomaterials often require a longer time to diffuse through the wetted layer and adsorb in a preferred orientation. If the time lapse between spraying and rinsing is shorter than the time scale for the diffusionadsorption process, then rinsing will dilute the concentration of the adsorbed species in the wetted film by partially washing away the non-adsorbed species, leading to poor layer growth. Additionally, a lack of layer interpenetration between PDAC and GO_{edge} leads to dissolution of the coating during spraying/ rinsing step as seen for (PDAC/GO_{Edge})₈₀ SA-LbL films [Fig. 3(a)]. Therefore, we replaced the rinsing step with blowdrying the film for 60 s between deposition steps. This not only eliminates the possibility of removal of non-adsorbed species from the wetted film but also results in a shorter diffusion length and faster adsorption due to the reduced thickness of the wetted film. Replacing rinsing with blow-drying led to deposition; however, the resulting deposition showed high roughness [Fig. 4(a)]. Even a reduced PDAC concentration (0.5 mg/ mL) and an extra rest time of 30 s between spraying and blowdrying did not improve the film homogeneity.

Therefore, we concluded that GO_{Edge} could not be deposited using SA-LbL assembly into homogeneous LbL coatings despite having a comparable zeta potential with PSS. The reason for this is that the even an extra rest time for the spray process is not sufficient for the adsorption of the GO_{Edge} in a preferred orientation owing to its rigid nanostructure and perhaps the absence of charged functional groups throughout the basal plane. This further emphasizes the importance of having a uniform charge distribution throughout the surface of nanomaterials for successful assembly of rigid nanomaterials with a spray-based approach.

Next, we moved our attention to SA-LbL using fully oxidized GO, which has a similar zeta potential arising from hydroxyl, epoxy, and carboxylic groups on the basal plane of the carbon framework. SA-LbL assembly was performed on (L-

Downloaded from https://www.cambridge.org/core. Texas A&M University Evans Libraries, on 17 Jul 2020 at 01:59:58, subject to the Cambridge Core terms of use, available at https://www.cambridge.org/core/terms. https://doi.org/10.1557/jmr.2020.44

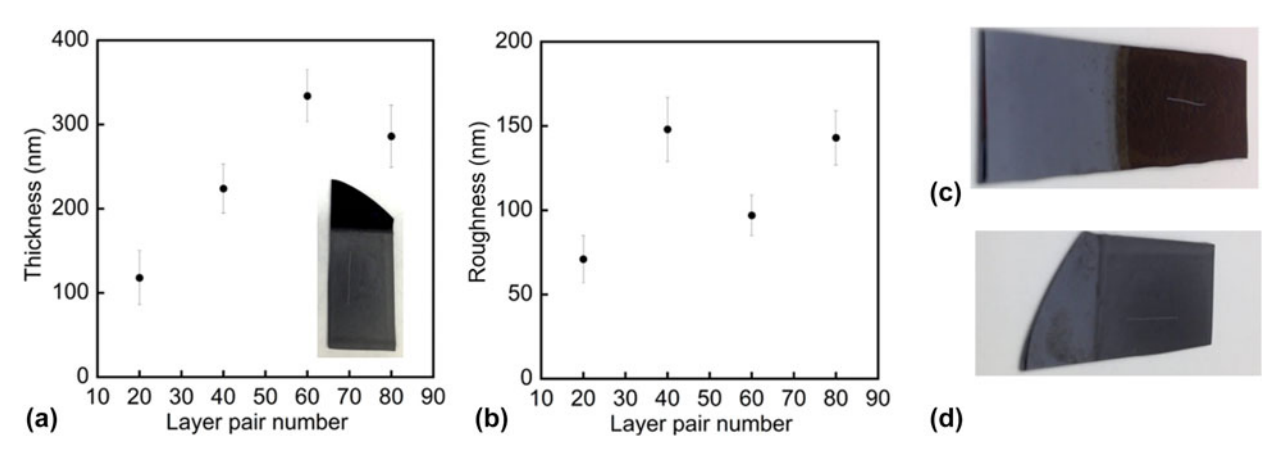


Figure 3: (a) Thickness and (b) roughness profiles of (LPEI/PAA)₄(PDAC/GO_{Edge})_n LbL films fabricated via SA-LbL assembly with alternate 10 s spraying and 10 s rinsing. The inset figure shows (LPEI/PAA)₄(PDAC/GO_{Edge})₆₀ film deposited by SA-LbL assembly. (c) Digital image of (PDAC/GO_{Edge})₁₅ LbL film fabricated by dipassisted LbL assembly. The resulting film had a thickness and roughness of 70 nm and 14 nm, respectively. (d) Digital image of (LPEI/PAA)₄ (PDAC/GO_{Edge})₂₀ LbL film fabricated by SA-LbL assembly. The resulting film possessed a thickness and roughness of 118 nm and 71 nm, respectively.

PEI/PAA)₄-coated silicon substrate using 10 s spray and 60 s of blow-drying for each step. When PDAC was used as the complementary species, the profilometric thickness for 60 bilayers of (PDAC/GO)60 LbL film was found to be 260 nm [Fig. 4(b)]. However, the resulting film possessed a high roughness of 190 nm, which was almost 75% of the overall film thickness [Fig. 4(c)]. The high roughness of the LbL film might arise from the high concentration of PDAC, which leads to adsorption of large amounts of GO for charge overcompensation resulting in island-like aggregation of GO in the film. We, therefore, employed a reduced PDAC concentration of 0.5 mg/mL without altering the GO concentration. This resulted compact and smoother (PDAC/GO) LbL films. For example, a 60-layer pair (PDAC/GO) LbL film possessed a thickness of 231 nm and roughness of 26 nm [Figs. 4(d) and 4(e)].

LbL assembly was originally established with rinsing between the deposition steps. Therefore, we decided to compare the effect of rinsing instead of blow-drying without altering the other parameters that had produced the lowroughness film. With 10 s of spray-rinsing in between the spray deposition steps, no coating was obtained except for some macroscopic accumulation at the bottom of the substrate [Fig. 4(f), right]. On the other hand, with blow-drying, homogeneous deposition was observed on the glass slide [Fig. 4(f), left]. Despite their comparable zeta potential values, PSS can be assembled with PDAC into an LbL film using SA-LbL assembly with a rinsing step, yet replacing PSS with GO does not give rise to any deposition. This further indicates that GO adsorption happens over a longer time scale and rinsing destroys the wetted film before the nanomaterials adsorb onto the surface. Additionally, despite the comparable zeta potential of GO and GO_{Edge}, the fact that only GO can be successfully assembled into an SA-LbL film with PDAC points out the

importance of uniform charge distribution throughout the nanomaterial framework. GO_{Edge} nanosheets have charged functional groups specifically at the edge of the carbon framework, whereas GO nanosheets have charged functional group randomly distributed throughout the basal plane.

From the results thus far, the following critical parameters are concluded to be important for SA-LbL assembly of anisotropic nanomaterials.

- (i) Presence of an adhesion-promoting layer,
- (ii) A stable and homogeneous dispersion of the nanomaterial,
- (iii) High absolute nanomaterial zeta potential, preferably on the face of the material,
- (iv) Low concentration of polymer (complementary species), and
- (v) Blow-drying instead of rinsing.

Next, we developed a library of (PDAC/GO)_n SA-LbL films and investigated their growth profiles, roughness, and surface morphology. First, the glass substrate was coated with (L-PEI/ PAA)₄ anchor layers using SA-LbL assembly (10 s spray and 10 s rinsing), followed by deposition of PDAC and GO by spraying the solution/dispersion for 10 s with 60 s of blowdrying in between the deposition steps. Figure 5(a) shows digital images of (PDAC/GO)_n SA-LbL films on glass substrates. With increasing number of deposition cycles, the glass slide turned more opaque, indicating successful deposition. A linear increase in the film thickness with the number of deposition cycles further confirms successful LbL deposition and is consistent with strong intermolecular interactions between PDAC and GO. The thickness increment was estimated to be 12 nm/layer pair from linear regression [Fig. 5(c)]. The roughness of the LbL film was obtained as the root mean square value measured using profilometry. Irrespective of the 📗 Journal of Materials Research 📗 Volume 35 📉 Issue 9 🖿 May 14, 2020 📗 www.mrs.org/jmi

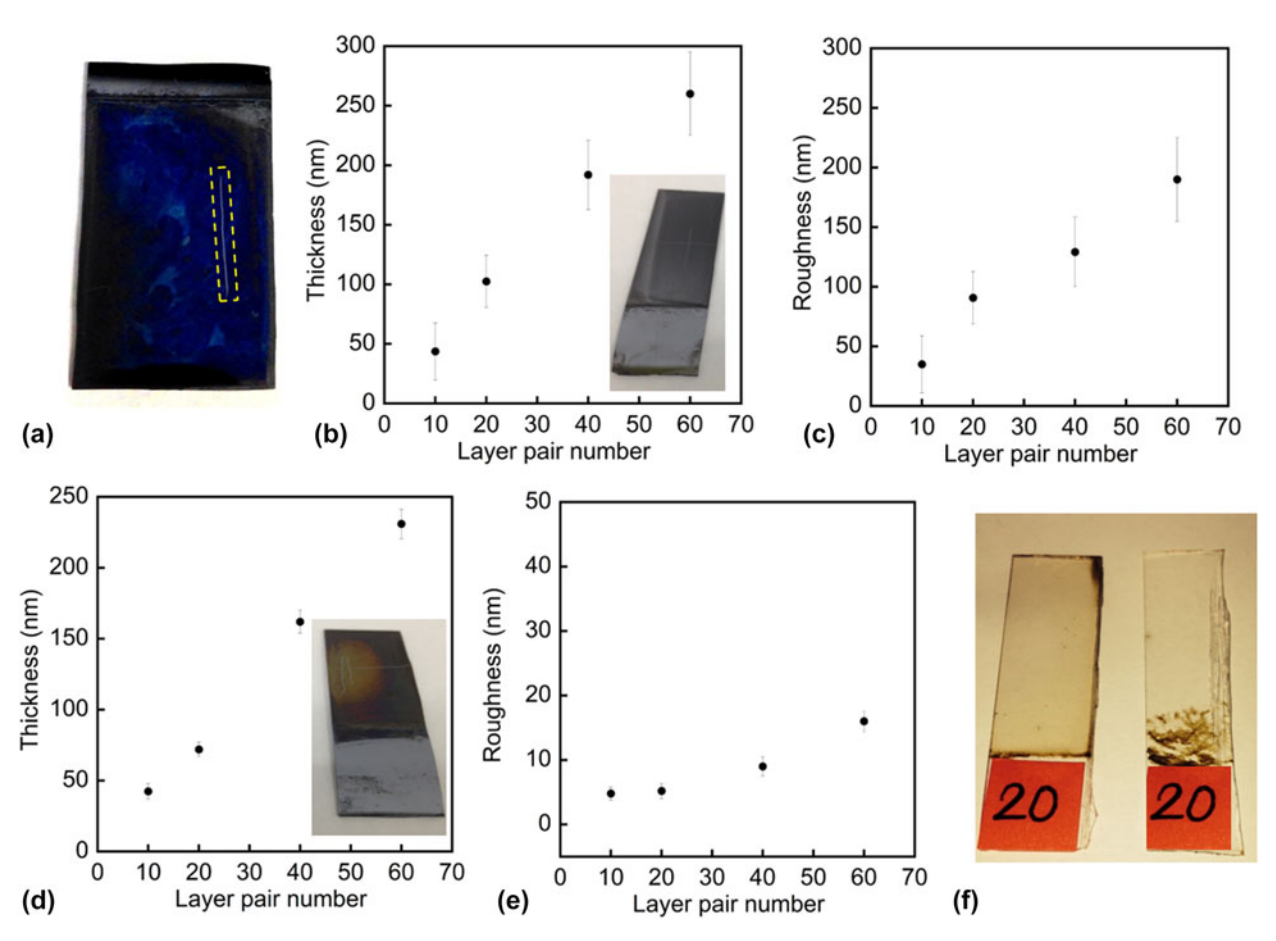


Figure 4: (a) (PDAC/GO_{Edge}) LbL film assembled using 10 s of spraying and 60 s of blow-drying. The thickness and roughness were measured across the scratch enclosed by the dotted square. The thickness and roughness of the film were 170 \pm 15 nm and 117 \pm 39 nm, respectively. The effect of polymer concentration on thickness and roughness of SA (PDAC/GO)_n LbL film constructed via 10 s of spraying and 60 s of blow-drying: (b) thickness and (c) roughness of LbL film deposited from 1 mg/mL PDAC on (L-PEI/PAA)₄-coated silicon substrate; (d) thickness and (e) roughness of LbL film deposited from 0.5 mg/mL PDAC on (L-PEI/PAA)₄-coated silicon substrate. The GO concentration was kept constant at 0.5 mg/mL. The inset figures in b and d are (L-PEI/PAA)₄(PDAC/GO)₆₀ SA-LbL film deposited on silicon substrate from 1 mg/mL and 0.5 mg/mL PDAC solution, respectively. (f) Effect of blow-drying (left) and rinsing (right) on spray assembled (PDAC/GO)₂₀ LbL films.

number of deposition cycles, the roughness values were considerably lower than the film thickness values, confirming homogeneous deposition and the nonporous nature of the coating. For example, the roughness of a (PDAC/GO)₆₀ LbL film was only 7% of its overall thickness [Fig. 5(d)]. The pinhole-free homogeneous deposition was further confirmed using optical microscopy imaging of the (PDAC/GO) LbL film [Fig. 5(b)]. The surface morphology of the LbL film was characterized using tapping-mode atomic force microscopy (AFM). Figures 5(e) and 5(f) represent the AFM height image of a (PDAC/GO)₁₀ LbL film and the section analysis, respectively. The discrepancy in the roughness obtained from profilometry (15 nm) and the AFM image (4.3 nm) was attributed to the length scale over which the measurements were carried out.

To demonstrate the versatility of the methodology, we prepared SA-LbL assembled films containing GO and a different polymer, branched polyethylenimine (B-PEI), using

identical spraying conditions. Figure 6(a) shows digital images of the $(B-PEI/GO)_n$ LbL films on the glass substrates. Similar to the $(PDAC/GO)_n$ system, the glass substrate became less transparent with an increasing number of deposition cycles. The (B-PEI/GO)_n LbL system follows linear growth behavior with a growth increment of 13.5 nm/layer pair [Fig. 6(c)]. The higher thickness increment for (B-PEI/GO) LbL film over (PDAC/GO) LbL film can be explained as follows: B-PEI is a weak polyelectrolyte containing primary, secondary, and tertiary amine groups having pK_a values of 4.5, 6.7, and 11.6, respectively [53, 54]. At lower pH values, B-PEI is extensively protonated, leading to an extended conformation due to charge-charge repulsion, resulting in compact LbL films. On the other hand, at higher pH (pH = 10), B-PEI is partially protonated and adopts a less extended conformation, which in turn leads to thicker LbL films [54, 55, 56]. Here, the assembly pH value for B-PEI was 10, which would lead to a slightly thicker film, as compared to PDAC. The profilometrically

📗 Journal of Materials Research 📗 Volume 35 📉 Issue 9 🖿 May 14, 2020 📗 www.mrs.org/jmi

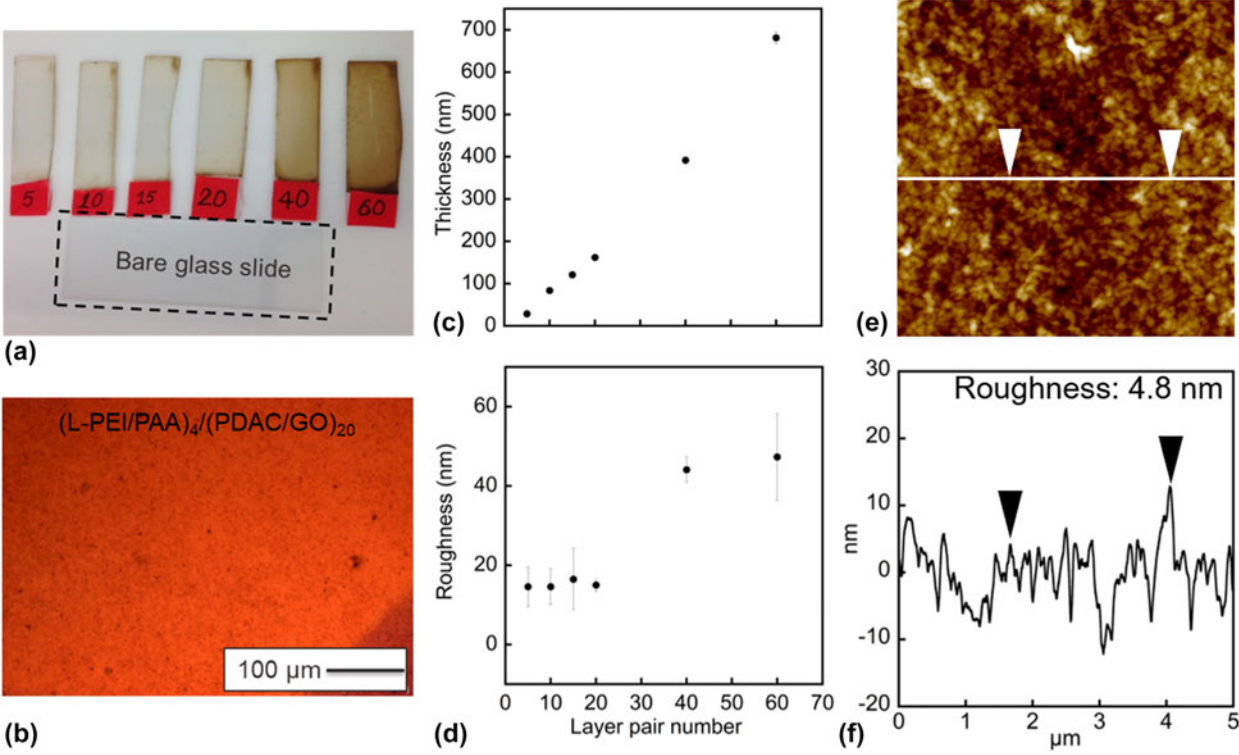


Figure 5: (a) Digital image of (PDAC/GO)_n SA-LbL film prepared by 10 s spraying and 60 s blow-drying for each exposure step. (b) Optical microscope image of (PDAC/GO)₂₀ SA-LbL film. Variation of (c) thickness and (d) roughness versus layer pair number for (PDAC/GO)_n SA-LbL film. (e) AFM height image of (PDAC/GO)₁₀ SA-LbL film. (f) Section analysis of the AFM image along the white line. All LbL films were deposited on (L-PEI/PAA)₄-coated glass substrates.

measured roughness values of the (B-PEI/GO) LbL films were considerably lower as than the overall thickness values [Fig. 6(d)]. For example, the roughness of a (B-PEI/GO)₄₀ LbL film was only 7% of the roughness value. The pinhole-free homogeneous deposition is further confirmed by the optical microscopy image of the LbL film [Fig. 6(b)]. Tapping-mode AFM was performed to analyze the surface morphology of the LbL film. Figures 6(e) and 6(f) represent the AFM height image and corresponding cross-section analysis of a (B-PEI/GO)₁₅ LbL film. Like the $(PDAC/GO)_n$ LbL system, the $(B-PEI/GO)_n$ LbL film showed similar microscopic morphology. The root mean square roughness of the (B-PEI/GO)_n LbL film was lower than that of (PDAC/GO)_n LbL film, indicating a slightly smoother surface of the former.

Conclusion

In summary, we have determined an optimum protocol to assemble anisotropic nanomaterials with polymers using SA-LbL assembly. We used GO as the anisotropic nanomaterial and PDAC or B-PEI as the polymeric component. Through systematic screening of different parameters, we show that the critical criteria for successful SA-LbL assembly are the stability of the dispersion, uniform charge on the face of the nanomaterial (as opposed to localized charge at the edge), an anchor layer that facilitates layer growth, and low polymer concentration to avoid aggregation of GO in the wetted layer. We have also established that blow-drying instead of rinsing in between the deposition steps promotes successful layer growth. We attributed this to the fact that rinsing destroys the GOcontaining wetted film by partially washing away the nonadsorbed species, leading to poor layer growth. On the other hand, blow-drying reduces the thickness of the wetted adsorbing layer, thereby facilitating the adsorption process. With these optimized conditions, it is possible to assemble polymer and GO sheets into smooth pinhole-free coatings using SA-LbL assembly, which was otherwise difficult to realize using the traditional SA-LbL approach used to assemble polyelectrolyte multilayers.

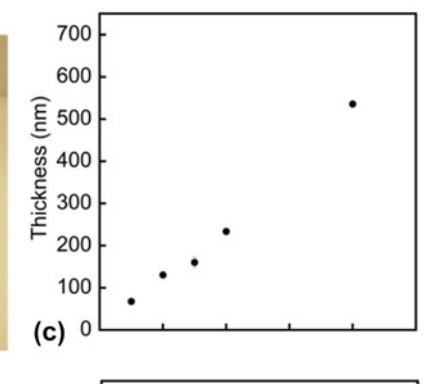
Experimental section

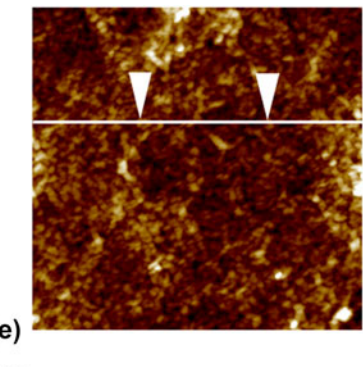
Materials

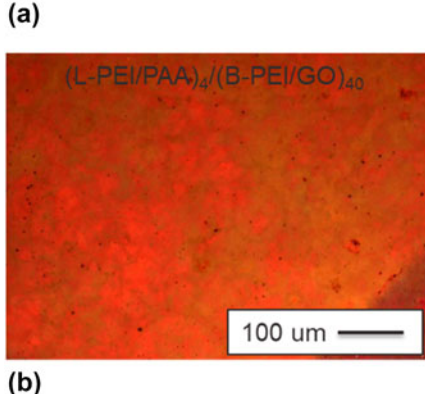
Graphite (SP-1) was purchased from Bay Carbon. Sodium nitrate, potassium permanganate, B-PEI ($M_{\rm w}=25{,}000~{\rm g/mol}$), PDAC ($M_{\rm w} = 200,000-350,000$ g/mol), and PAA ($M_{\rm w} =$ 50,000 g/mol) were purchased from Sigma Aldrich. L-PEI ($M_{\rm w}$ = 25,000 g/mol) was purchased from Polyscience. All the polymers were used as received without any further purification. GO_{Edge} was obtained from Garmor and used as received.

🔳 Journal of Materials Research 📗 Volume 35 🔳 Issue 9 🖿 May 14, 2020 🔳 www.mrs.org/jmr



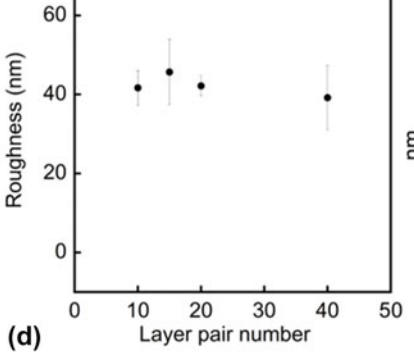






15

20



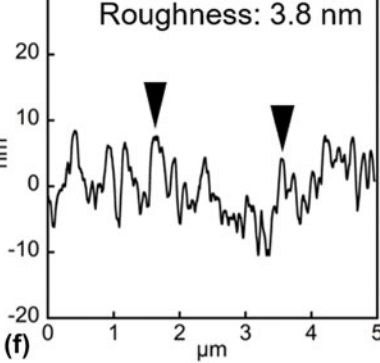


Figure 6: (a) Digital image of (B-PEI/GO)_n SA-LbL film prepared by 10 s spraying and 60 s blow-drying. (b) Optical microscope image of (B-PEI/GO)₄₀ LbL film. Variation of (c) thickness and (d) roughness versus layer pair number for (B-PEI/GO)_n SA-LbL film. (e) AFM height image of (B-PEI/GO)₁₅ SA-LbL film. (f) Section analysis of AFM image along the white line. All the LbL films were deposited on (L-PEI/PAA)₄-coated glass substrates.

Preparation of graphite oxide

GO was prepared according to a modified Hummers' method [57]. In brief, 3 g of graphite powder and 2.5 g of NaNO₃ were added to cold concentrated sulfuric acid and the mixture was stirred for 5 h in an ice bath. 15 g of KMnO₄ was next added slowly into the mixture. During the addition, the mixture was stirred continuously and kept in an ice bath to maintain the temperature below 20 °C. After that, 200 mL of deionized (DI) water was added approximately at a rate of 5 mL/min into the solution mixture while keeping the mixture in the ice bath. Then, 700 mL of DI water was poured into the mixture and stirred approximately for 30 min, followed by addition of 20 mL of 30% H₂O₂. Upon the addition of H₂O₂, the reaction mixture turned brown. The mixture was continuously stirred for 30 more minutes. The reaction mixture was then washed with 1 L of 5 wt% HCl, followed twice with DI water. Finally, the mixture was filtered through Whatman filter paper (pore size 2.5 µm, diameter 55 mm). The filtered graphite oxide cake was redispersed in DI water and dialyzed. Upon completion of the dialysis, the resulting dispersion was dried in a convection oven at 60 °C to obtain dried GO.

Solution/dispersion preparation for LbL assembly

Aqueous solutions of L-PEI (positively charged polyelectrolyte) and PAA (negatively charged polyelectrolyte) were prepared with a concentration of 20 mM based on the molar mass of the repeat unit. The pH of both solutions was adjusted to 4. GO and $\mathrm{GO}_{\mathrm{Edge}}$ were added to DI water and exfoliated via ultrasonication to obtain 0.5 mg/mL dispersion. The pH of both dispersions was adjusted to 3.5. These dispersions were later bath sonicated prior to use. B-PEI aqueous solution was prepared at a concentration of 0.5 mg/mL, followed by pH adjustment to 10. PDAC aqueous solution of concentration of 0.5 mg/mL and 1.0 mg/mL was prepared without any pH adjustment.

30

LbL assembly

LbL assembly was carried out on silicon and glass substrates. Both substrates were treated with basic piranha solution (5:1:1 H₂O, 30 wt% NH₃ and 30 wt% H₂O₂, respectively) at 70 °C for 15 min, followed by thorough rinsing with DI water (Caution: piranha solution is highly corrosive and proper precaution must be taken while handing). The cleaned substrates were stored in DI water until used. Before use, the substrate was dried with a stream of nitrogen and exposed to oxygen plasma for 5 min and immediately subjected to SA-LbL assembly using an automated spraying machine (Svaya Nanotechnology Inc.). All LbL films were assembled at a constant pressure of 30 psi, and the distance between the spray nozzle and the substrate was maintained at 7.25 inches.

🔳 Journal of Materials Research 📗 Volume 35 🖿 Issue 9 🖿 May 14, 2020 💻 www.mrs.org/jmi





Characterization

Thickness and roughness were measured using a profilometer (P-6; KLA-Technor). The average of five different measurements was taken as the film thickness. AFM measurements were carried out using a Bruker Dimension Icon AFM under tapping mode. Optical microscopy image was obtained using Axio Imager A1m (Carl Zeiss). Zeta potential measurements was carried out using Zetasizer ZS90 particle size and zeta potential analyzer (Malvern Instruments).

Acknowledgment

We thank the Materials Characterization Facility at Texas A&M University. This work was supported by the National Science Foundation (Grant No. 1905732) (J.L.L.). S.D. thanks the support from Collaborative Research Scheme, MHRD, Government of India.

References

- 1. G. Decher, J.D. Hong, and J. Schmitt: Buildup of ultrathin multilayer films by a self-assembly process: III. Consecutively alternating adsorption of anionic and cationic polyelectrolytes on charged surfaces. Thin Solid Films 210-211, 831 (1992).
- 2. G. Decher: Fuzzy nanoassemblies: Toward layered polymeric multicomposites. Science 277, 1232 (1997).
- 3. J.J. Richardson, M. Björnmalm, and F. Caruso: Technologydriven layer-by-layer assembly of nanofilms. Science 348, aaa2491
- 4. G. Nabar, M. Souva, K.H. Lee, S. De, J. Lutkenhaus, B. Wyslouzil, and J.O. Winter: High-throughput nanomanufacturing via spray processes. In Nanotechnology Commercialization Edited by T.O. Mensah, B. Wang, G. Bothun, J. Winter and V. Davis, (John Wiley & Sons, Inc., USA, 2017); p. 101.
- 5. J-W. Jeon, S.R. Kwon, and J.L. Lutkenhaus: Polyaniline nanofiber/electrochemically reduced graphene oxide layer-by-layer electrodes for electrochemical energy storage. J. Mater. Chem. A. 3, 3757 (2015).
- 6. T. Guin, M. Krecker, A. Milhorn, D.A. Hagen, B. Stevens, and J.C. Grunlan: Exceptional flame resistance and gas barrier with thick multilayer nanobrick wall thin films. Adv. Mater. Interfaces 2, 1500214 (2015).
- 7. C.M. Andres, I. Larraza, T. Corrales, and N.A. Kotov: Nanocomposite microcontainers. Adv. Mater. 24, 4597 (2012).
- 8. L. Escobar-Ferrand, D. Li, D. Lee, and C.J. Durning: Allnanoparticle layer-by-layer surface modification of micro-and ultrafiltration membranes. Langmuir 30, 5545 (2014).
- 9. G.S. Lee, Y-J. Lee, and K.B. Yoon: Layer-by-layer assembly of zeolite crystals on glass with polyelectrolytes as ionic linkers. J. Am. Chem. Soc. 123, 9769 (2001).

- 10. Y. Kang, L. Emdadi, M.J. Lee, D. Liu, and B. Mi: Layer-by-layer assembly of zeolite/polyelectrolyte nanocomposite membranes with high zeolite loading. Environ. Sci. Technol. Lett. 1, 504 (2014).
- 11. S. De, M.I. Nandasiri, H.T. Schaef, B.P. McGrail, S.K. Nune, and J.L. Lutkenhaus: Water-based assembly of polymer-metal organic framework (MOF) functional coatings. Adv. Mater. Interfaces 4, 1600905 (2016).
- 12. K.C. Krogman, J.L. Lowery, N.S. Zacharia, G.C. Rutledge, and P.T. Hammond: Spraying asymmetry into functional membranes layer-by-layer. Nat. Mater. 8, 512 (2009).
- 13. T. Sasaki, Y. Ebina, T. Tanaka, M. Harada, M. Watanabe, and G. Decher: Layer-by-layer assembly of titania nanosheet/ polycation composite films. Chem. Mater. 13, 4661 (2001).
- 14. A. Qi, P. Chan, J. Ho, A. Rajapaksa, J. Friend, and L. Yeo: Template-free synthesis and encapsulation technique for layer-bylayer polymer nanocarrier fabrication. ACS Nano 5, 9583 (2011).
- 15. J.L. Lutkenhaus, K.D. Hrabak, K. McEnnis, and P.T. Hammond: Elastomeric flexible free-standing hydrogen-bonded nanoscale assemblies. J. Am. Chem. Soc. 127, 17228 (2005).
- 16. G.B. Sukhorukov, J. Schmitt, and G. Decher: Reversible swelling of polyanion/polycation multilayer films in solutions of different ionic strength. Bunsen-Ges. Phys. Chem., Ber. 100, 948 (1996).
- 17. Y. Lvov, H. Haas, G. Decher, H. Moehwald, and A. Kalachev: Assembly of polyelectrolyte molecular films onto plasma-treated glass. J. Phys. Chem. 97, 12835 (1993).
- 18. P. Lavalle, C. Gergely, F.J.G. Cuisinier, G. Decher, P. Schaaf, J.C. Voegel, and C. Picart: Comparison of the structure of polyelectrolyte multilayer films exhibiting a linear and an exponential growth regime: An in situ atomic force microscopy study. Macromolecules 35, 4458 (2002).
- 19. A. Izquierdo, S.S. Ono, J.C. Voegel, P. Schaaf, and G. Decher: Dipping versus spraying: exploring the deposition conditions for speeding up layer-by-layer assembly. Langmuir 21, 7558 (2005).
- 20. J. Zhu, H. Zhang, and N.A. Kotov: Thermodynamic and structural insights into nanocomposites engineering by comparing two materials assembly techniques for graphene. ACS Nano 7, 4818 (2013).
- 21. R. Merindol, S. Diabang, O. Felix, T. Roland, C. Gauthier, and G. Decher: Bio-inspired multiproperty materials: Strong, selfhealing, and transparent artificial wood nanostructures. ACS Nano 9, 1127 (2015).
- 22. F. Xiang, D. Parviz, T.M. Givens, P. Tzeng, E.M. Davis, C.M. Stafford, M.J. Green, and J.C. Grunlan: Stiff and transparent multilayer thin films prepared through hydrogenbonding layer-by-layer assembly of graphene and polymer. Adv. Funct. Mater. 26, 2143 (2016).
- 23. T. Guin, B. Stevens, M. Krecker, J. D'Angelo, M. Humood, Y. Song, R. Smith, A. Polycarpou, and J.C. Grunlan: Ultrastrong, chemically resistant reduced graphene oxide-based multilayer thin



- films with damage detection capability. ACS Appl. Mater. Interfaces **8**, 6229 (2016).
- 24. S. Qin, M.G. Pour, S. Lazar, O. Köklükaya, J. Gerringer, Y. Song, L. Wågberg, and J.C. Grunlan: Super gas barrier and fire resistance of nanoplatelet/nanofibril multilayer thin films. Adv. Mater. Interfaces 6, 1801424 (2019).
- **25. J.B. Schlenoff, S.T. Dubas, and T. Farhat**: Sprayed polyelectrolyte multilayers. *Langmuir* **16**, 9968 (2000).
- 26. C. Lu, I. Dönch, M. Nolte, and A. Fery: Au nanoparticle-based multilayer ultrathin films with covalently linked nanostructures: Spraying layer-by-layer assembly and mechanical property characterization. *Chem. Mater.* 18, 6204 (2006).
- K.C. Krogman, N.S. Zacharia, S. Schroeder, and
 P.T. Hammond: Automated process for improved uniformity and versatility of layer-by-layer deposition. *Langmuir* 23, 3137 (2007).
- 28. G.M. Nogueira, D. Banerjee, R.E. Cohen, and M.F. Rubner: Spray-layer-by-layer assembly can more rapidly produce optical-quality multistack heterostructures. *Langmuir* 27, 7860 (2011).
- P.C. Suarez-Martinez, J. Robinson, H. An, R.C. Nahas,
 D. Cinoman, and J.L. Lutkenhaus: Spray-on polymer-clay multilayers as a superior anticorrosion metal pretreatment.
 Macromol. Mater. Eng. 302, 1600552 (2017).
- S.R. Kwon, J-W. Jeon, and J.L. Lutkenhaus: Sprayable, paintable layer-by-layer polyaniline nanofiber/graphene electrodes. *RSC Adv.* 5, 14994 (2015).
- R. Blell, X. Lin, T. Lindström, M. Ankerfors, M. Pauly, O. Felix, and G. Decher: Generating in-plane orientational order in multilayer films prepared by spray-assisted layer-by-layer assembly. ACS Nano 11, 84 (2017).
- J.T. O'Neal, M.J. Bolen, E.Y. Dai, and J.L. Lutkenhaus:
 Hydrogen-bonded polymer nanocomposites containing discrete layers of gold nanoparticles. *J. Colloid Interface Sci.* 485, 260 (2017).
- 33. H. Hu, M. Pauly, O. Felix, and G. Decher: Spray-assisted alignment of layer-by-layer assembled silver nanowires: A general approach for the preparation of highly anisotropic nano-composite films. Nanoscale 9, 1307 (2017).
- **34. J. Heo, M. Choi, and J. Hong**: Facile surface modification of polyethylene film via spray-assisted layer-by-layer self-assembly of graphene oxide for oxygen barrier properties. *Sci. Rep.* **9**, 2754 (2019)
- M.Q. Zhao, N. Trainor, C.E. Ren, M. Torelli, B. Anasori, and Y. Gogotsi: Scalable manufacturing of large and flexible sheets of MXene/graphene heterostructures. *Adv. Mater. Technol.* 4, 1800639 (2019).
- 36. A. Rani, K. Chung, J. Kwon, S.J. Kim, Y.H. Jang, Y.J. Jang, L.N. Quan, M. Yoon, J.H. Park, and D.H. Kim: Layer-by-layer self-assembled graphene multilayers as Pt-free alternative counter electrodes in dye-sensitized solar cells. ACS Appl. Mater. Interfaces 8, 11488 (2016).

- J. Hong and S.W. Kang: Carbon decorative coatings by dip-, spin-, and spray-assisted layer-by-layer assembly deposition. *J. Nanosci.* Nanotechnol. 11, 7771 (2011).
- 38. S. De, C. Purcell, J. Murley, P. Flouda, S. Shah, M. Green, and J. Lutkenhaus: Spray-on reduced graphene oxide–poly(vinyl alcohol) supercapacitors for flexible energy and power. *Adv. Mater. Interfaces* 5, 1801237 (2018).
- 39. B. Stevens, E. Dessiatova, D.A. Hagen, A.D. Todd, C.W. Bielawski, and J.C. Grunlan: Low-temperature thermal reduction of graphene oxide nanobrick walls: Unique combination of high gas barrier and low resistivity in fully organic polyelectrolyte multilayer thin films. ACS Appl. Mater. Interfaces 6, 9942 (2014).
- **40.** Y.H. Yang, L. Bolling, M.A. Priolo, and J.C. Grunlan: Super gas barrier and selectivity of graphene oxide-polymer multilayer thin films. *Adv. Mater.* **25**, 503 (2013).
- **41. S. De and J.L. Lutkenhaus**: Corrosion behaviour of eco-friendly airbrushed reduced graphene oxide–poly(vinyl alcohol) coatings. *Green Chem.* **20**, 506 (2018).
- 42. R. Xiong, K. Hu, A.M. Grant, R. Ma, W. Xu, C. Lu, X. Zhang, and V.V. Tsukruk: Ultrarobust transparent cellulose nanocrystal-graphene membranes with high electrical conductivity. *Adv. Mater.* 28, 1501 (2016).
- **43. D. Zhang, J. Tong, and B. Xia**: Humidity-sensing properties of chemically reduced graphene oxide/polymer nanocomposite film sensor based on layer-by-layer nano self-assembly. *Sens. Actuators, B* **197**, 66 (2014).
- 44. D. Zhang, J. Tong, B. Xia, and Q. Xue: Ultrahigh performance humidity sensor based on layer-by-layer self-assembly of graphene oxide/polyelectrolyte nanocomposite film. Sens. Actuators, B 203, 263 (2014).
- C. Sellam, Z. Zhai, H. Zahabi, O.T. Picot, H. Deng, Q. Fu,
 E. Bilotti, and T. Peijs: High mechanical reinforcing efficiency of layered poly(vinyl alcohol)–graphene oxide nanocomposites.
 Nanocomposites 1, 89 (2015).
- 46. S-M. Lee, H. Jeong, N.H. Kim, H-G. Kim, and J.H. Lee: Layer-by-layer assembled graphene oxide/polydiallydimethylammonium chloride composites for hydrogen gas barrier application. Adv. Compos. Mater. 27, 457 (2018).
- 47. C. Vallés, X. Zhang, J. Cao, F. Lin, R.J. Young, A. Lombardo, A.C. Ferrari, L. Burk, R. Mülhaupt, and I.A. Kinloch: Graphene/ polyelectrolyte layer-by-layer coatings for electromagnetic interference shielding. ACS Appl. Nano Mater. 2, 5272 (2019).
- 48. Y. Akgöl, C. Cramer, C. Hofmann, Y. Karatas, H-D. Wiemhöfer, and M. Schönhoff: Humidity-Dependent DC conductivity of polyelectrolyte multilayers: Protons or other small ions as charge carriers? *Macromolecules* 43, 7282 (2010).
- **49. S.T. Dubas and J.B. Schlenoff**: Polyelectrolyte multilayers containing a weak polyacid: Construction and deconstruction. *Macromolecules* **34**, 3736 (2001).



- 50. N. Ladhari, J. Hemmerlé, C. Ringwald, Y. Haikel, J-C. Voegel, P. Schaaf, and V. Ball: Stratified PEI-(PSS-PDADMAC)₂₀-PSS-(PDADMAC-TiO₂)_n multilayer films produced by spray deposition. *Colloids Surf.*, A 322, 142 (2008).
- 51. N. Ladhari, J. Hemmerlé, Y. Haikel, J-C. Voegel, P. Schaaf, and V. Ball: Stability of embossed PEI-(PSS-PDADMAC)₂₀ multilayer films versus storage time and versus a change in ionic strength. *Appl. Surf. Sci.* 255, 1988 (2008).
- 52. L. Wågberg, G. Decher, M. Norgren, T. Lindström, M. Ankerfors, and K. Axnäs: The build-up of polyelectrolyte multilayers of microfibrillated cellulose and cationic polyelectrolytes. *Langmuir* 24, 784 (2008).
- 53. I. Willner, Y. Eichen, A.J. Frank, and M.A. Fox: Photoinduced electron-transfer processes using organized redox-functionalized

- bipyridinium-polyethylenimine-titania colloids and particulate assemblies. *J. Phys. Chem.* **97**, 7264 (1993).
- 54. Y. Gu, Y. Ma, B.D. Vogt, and N.S. Zacharia: Contraction of weak polyelectrolyte multilayers in response to organic solvents. *Soft Matter* 12, 1859 (2016).
- 55. S.S. Shiratori and M.F. Rubner: pH-dependent thickness behavior of sequentially adsorbed layers of weak polyelectrolytes. Macromolecules 33, 4213 (2000).
- 56. B. Stevens, T. Guin, O. Sarwar, A. John, K.R. Paton, J.N. Coleman, and J.C. Grunlan: Highly conductive graphene and polyelectrolyte multilayer thin films produced from aqueous suspension. *Macromol. Rapid Commun.* 37, 1790 (2016).
- **57. W.S. Hummers and R.E. Offeman**: Preparation of graphitic oxide. *J. Am. Chem. Soc.* **80**, 1339 (1958).